4. Bellomo R, Farmer M, Wong C, Boyce N. A prospective study of technetium-99m-diethylenetriamine pentaacetic acid renal allograft scintigraphy in the diagnostic evaluation of graft dysfunction. *Transplantation* 1993;56:1585–1588.
5. Fommei E, Volterrani D. Renal nuclear medicine. *Semin Nucl Med* 1995;25:183–194.
6. Gratz KF. Functional scintigraphy in the follow-up of transplants. *Nuklearmedizin* 1993;32:215–220.
7. Pouteil-Noble C, Yatim A, Najem R, Colon S, Peyrin JO, Touraine JL. Diagnostic value of [99mTc]MAG3 imaging in the oligoanuria of the renal transplant patient in the first month after transplantation. *Transplant Proc* 1994;26:303–304.
8. Sayman HB, Sonmezoglu K, Ayaz M, Kahraman N, Kapicioglu T, Urgancioglu I. Functional evaluation of renal transplants with scintigraphy. *J Nucl Biol Med* 1993;37:115–118.
9. Pjura GA, Kim EE, Lowry PA, Verani RR, Kahan BD, Crews LD. Radionuclide differentiation of acute cellular rejection from cyclosporin nephrotoxicity. *Contrib Nephrol* 1987;56:163–167.
10. Riccabona G, Fill H, Hilty E, Leidlmair K. Prognosis of renal transplant function by renography with radioactive hippuran. *Uremia Invest* 1985;9:281–285.
11. Clorius JH, Dreikorn K, Schmidlin P, Orthgiess H. Prognostic value of post-transplant hippurate scintigraphy. *J Urol* 1983;129:920–924.
12. Dahlager JI, Bilde T. The ^{125}I-Hippuran renogram in rabbit kidneys after graded warm ischemia. *Scand J Urol Nephrol* 1980;14:85–90.
13. Dahlager JI, Bilde T. The uptake of hippuran in kidney slices employed as a viability test. *Scand J Urol Nephrol* 1976;10:120–125.
14. Gifford RR, Neuymer MM, Yang HC, Escobar FS, Thiele BL. Successful identification of acute renal allograft rejection with duplex ultrasonography. *Clin Transplant* 1994;8:40–44.
15. Kirchner PT, Goldman MH, Leapman SB, Kiepfer RF. Clinical application of the kidney to aortic blood flow index (K/A ratio). *Contrib Nephrol* 1978;11:120–126.
16. Hibberd PL, Rubin RH. Renal transplantation and related infections. *Semin Respir Infect* 1993;8:216–224.
17. Abdel-Sayed FI, Stewart TH. A case of "cold" white kidney. *Can Med Assoc J* 1973;109:352.
18. Fernando DC, Young KC. Scintigraphic patterns of acute vascular occlusion following renal transplantation. *Nucl Med Commun* 1986;7:223–231.
19. Freedman GS, Schiff M, Zager P, Jones D, Hausman M. The temporal and pathological significance of perfusion failure following renal transplantation. *Radiology* 1975;114:649–654.
20. Bouvier JF, Garnier JL, Chauvot P, et al. The hyperactive halo as a sign of renal graft death in ^{99m}Tc-DTPA studies. *Eur J Nucl Med* 1983;8:555–556.
21. Lubin E, Shapira Z, Melloul M, Youssim A. Scintigraphic detection of vascular and urological complications in the transplanted kidney: 133 cases. *Eur J Nucl Med* 1985;10:313–316.
22. Shih WJ, Coleman RC, Mitchell B, Munch LC. Enlarged photon-deficient area in expected site of renal allograft on Tc-99m-DTPA study. A sign of renal vein thrombosis. *Clin Nucl Med* 1993;18:974–997.
23. Jorgensen JI, Ladefoged J. The influence of ischemia on ^{131}I-hippuran renograms performed after kidney transplantation and its prognostic value. *Dan Med Bull* 1987;34:52–57.
24. Kjellstrand CM, Casali RE, Simmons RL, Shideman JR, Buselmeier TJ, Najarian JS. Etiology and prognosis in acute post-transplant renal failure. *Am J Med* 1976;61:190–199.
25. Staab EV, Kelly WD, Loken MK. Prognostic value of radioisotope renograms in kidney transplantation. *J Nucl Med* 1969;10:133–135.
26. Maher FT, Elveback LR. Simultaneous renal clearances of ^{125}I- and ^{131}I-labeled orthoiodohippurate and para-aminohippurate in the estimation of effective renal plasma flow in man. *Mayo Clin Proc* 1970;45:657–661.
27. Mushmov D, Brailska M, Budevski G, Salambashev L, Dimitrova S. Comparative studies on the determination of the differential effective renal plasma flow with ^{131}I-hippuran and PAH. *Int Urol Nephrol* 1973;5:205–208.
28. McAfee JG, Grossman ZD, Gagne G, et al. Comparison of renal extraction efficiencies for radioactive agents in the normal dog. *J Nucl Med* 1981;22:333–338.
29. Dahlager JI, Bilde T. Renographic evaluation of kidney preservation with chlorpromazine. *J Nucl Med* 1979;20:18–25.
30. Lannon SG, Bickis I, Dossetor JB. Viability testing of kidneys for transplantation. *Invest Urol* 1971;9:180–183.
31. Lin EC, Gellens ME, Goodgold HM. Prognostic value of renal scintigraphy with ^{99m}Tc-MAG3 in patients with acute renal failure [Abstract]. *J Nucl Med* 1995; 36(suppl):232P–233P.
32. Duckett T, Bretan PN Jr, Cochran ST, Rajfer J, Rosenthal JT. Noninvasive radiological diagnosis of renal vein thrombosis in renal transplantation. *J Urol* 1991;146:403–406.
33. Borowicz MR, Hanevold CD, Cofer JB, Bromberg JS, Orak JK, Rajagopalan PR. Extrinsic compression in the iliac fossa can cause renal vein occlusion in pediatric kidney recipients, but graft loss can be prevented. *Transplant Proc* 1994;26:119–120.

MAG3 SPECT: A Rapid Procedure to Evaluate the Renal Parenchyma

George N. Sfakianakis and Mike F. Georgiou
Division of Nuclear Medicine, Department of Radiology and Department of Pediatrics, University of Miami School of Medicine/Jackson Memorial Hospital, Miami, Florida

Renal parenchymal (cortical) scintigraphy (planar or SPECT) is indicated for the diagnosis and follow-up of focal functional disorders, such as acute pyelonephritis, and for accurate quantitation of split renal function, especially in cases of atypical location of the kidney(s). This static imaging procedure is currently performed 3–5 hr after the injection of a cortical fixation agent, ^{99m}Tc-DMSA or ^{99m}Tc-GH, and requires effective immobilization of the patient for 30 min. **Methods:** In five healthy adult volunteers and five children with various clinical indications, SPECT renal parenchymal scintigraphy was performed with a three-detector camera in 1-min per revolution sequential intervals for a total acquisition time of 4 min, beginning immediately after an intravenous injection of a graduated dose of 20 mCi (minimum 2 mCi) of the dynamic renal agent ^{99m}Tc-MAG3. **Results:** Tomograms of the renal parenchyma reconstructed in three projections and volume-rendered reprojection of the SPECT-volume data indicated normal or abnormal renal parenchyma. Comparisons were made with planar MAG3 and SPECT-GH and favored MAG3-SPECT. However, comparisons with DMSA indicated certain disadvantages of MAG3 SPECT. For most organs, the radiation dose estimates from 20 mCi MAG3 were lower than those from DMSA (6 mCi) or GH (20 mCi). Simultaneous injection of MAG3 and a diuretic (2–40 mg furosemide) resulted in lower than usually reported radiation dose estimates for the urinary bladder (target organ) and the gonads, and allowed subsequent evaluation of the drainage system. **Conclusion:** MAG3 SPECT is feasible, clinically useful and may be offered as a rapid (4 min) renal parenchymal imaging procedure, or it may precede planar dynamic (diuretic) MAG3 scintigraphy.

Key Words: renal parenchymal scintigraphy; SPECT; technetium-99m-MAG3; acute pyelonephritis; ectopic kidney; growth-arrested kidney; split renal function

J Nucl Med 1997; 38:478–483

High-resolution renal parenchymal (cortical) scintigraphy is indicated for the diagnosis and follow-up of focal (functional or anatomical) disorders of the kidneys, primarily acute pyelonephritis and scars, especially in children (*1–9*). It is also useful in evaluating the split renal function, particularly in cases of renal ectopia, in certain renal axis deviations, and in ptotic or wandering kidneys (*10–14*). Currently, the technique of choice for renal parenchymal scintigraphy is static late imaging 3–6 hr after an intravenous injection of a cortical fixation agent, ^{99m}Tc-glucoheptonate (GH) or ^{99m}Tc-dimercaptosuccinic acid (DMSA). Imaging is usually performed in planar mode and

Received Dec. 8, 1995; revision accepted June 15, 1996.
For correspondence or reprints contact: George N. Sfakianakis, MD, Division of Nuclear Medicine (D-57), University of Miami School of Medicine, P.O. Box 016960, Miami, FL 33101.

multiple projections with parallel or pinhole collimation or, less frequently, in SPECT mode with multidetector cameras and high-resolution, parallel-hole collimation (*9*). The duration of imaging sessions ranges between 30–60 min.

Technetium-99m-mertiatide (MAG3) is, primarily, a tubular renal imaging agent and is used for planar dynamic studies to assess global renal parenchymal flow and function and to determine drainage adequacy of the kidneys (*15–16*). MAG3 dynamic studies do not require a waiting period after injection of the radiopharmaceutical and their acquisition time is 20–30 min. However, due to its high extraction efficiency, MAG3 provides high-resolution parenchymal images 1–4 min after injection and may be suitable for renal parenchymal (cortical) scintigraphy. Some investigators have evaluated the use of planar dynamic MAG3 scintigraphy for investigating the renal parenchyma in urinary tract infection (UTI) patients. Variable results were reported in different studies (*17–20*). In our experience, the lack of three-dimensional information appears to have a negative effect on the specificity of planar MAG3 dynamic imaging in the investigation of focal lesions of the renal parenchyma (*20*). This prompted the evaluation of MAG3 for SPECT studies. In this article, we report our initial observations on the feasibility of a rapid renal parenchymal SPECT with MAG3 in normal adult volunteers and in children with UTI or other renal parenchymal clinical problems.

MATERIALS AND METHODS

Patients

Ten patients were studied: five healthy adult volunteers, appropriately informed, and five children with normal global renal function (by plasma creatinine levels) and clinical indications for renal parenchymal evaluation. One of the volunteers, with a history of UTIs, had a DMSA-SPECT 2 yr previously. The five children were studied with SPECT-MAG3 due to nonavailability of DMSA and to obtain clinically needed renal parenchymal information. Three infants (1–6 mo old) with UTI were evaluated for obstruction with planar MAG3 scintigraphy, which indicated unilateral or bilateral cortical areas with decreased function, suspicious for acute pyelonephritis (APN). The fourth child, with a past history of UTI, was evaluated for renal cortical anatomy and split function with a GH-SPECT, that, despite hydration and diuretics, was suboptimal due to collecting system retention of activity. A 6-day-old infant with an ectopic kidney by planar MAG3, was studied to assure accurate measurement of the split renal function, which could not be obtained with the planar study due to different location and attenuation of the kidneys.

Methods

Commercially available betiatide in a kit form (TechneScan MAG3, Mallinckrodt Medical Inc., St. Louis, MO) was labeled with freshly eluted ^{99m}Tc-pertechnetate to prepare ^{99m}Tc-mertiatide (MAG3). For this protocol, the adult dose was 20 mCi (740 MBq) and the pediatric dose was calculated according to body weight using the formula 20 mCi × weight/70 kg (or 150 lb). The minimum dose injected was 2 mCi (74 MBq). Immediately after the injection of the radiopharmaceutical, all patients received an intravenous dose of 1 mg/kg, maximum 40 mg, furosemide (Lasix). Timing of bladder voiding was reported by the volunteers and was observed and recorded in the children.

Imaging was performed using a three-detector camera (Triad, Trionix Laboratories, Twinsburg, OH). After oral hydration (targeting an optimum 10 ml/kg), the patient was appropriately positioned inside the gantry of the three-detector camera and was restricted, as needed, without sedation. An indwelling needle (butterfly) was inserted into an antecubital vein and tested for leaks. Acquisition was initiated immediately before the injection of MAG3 and furosemide.

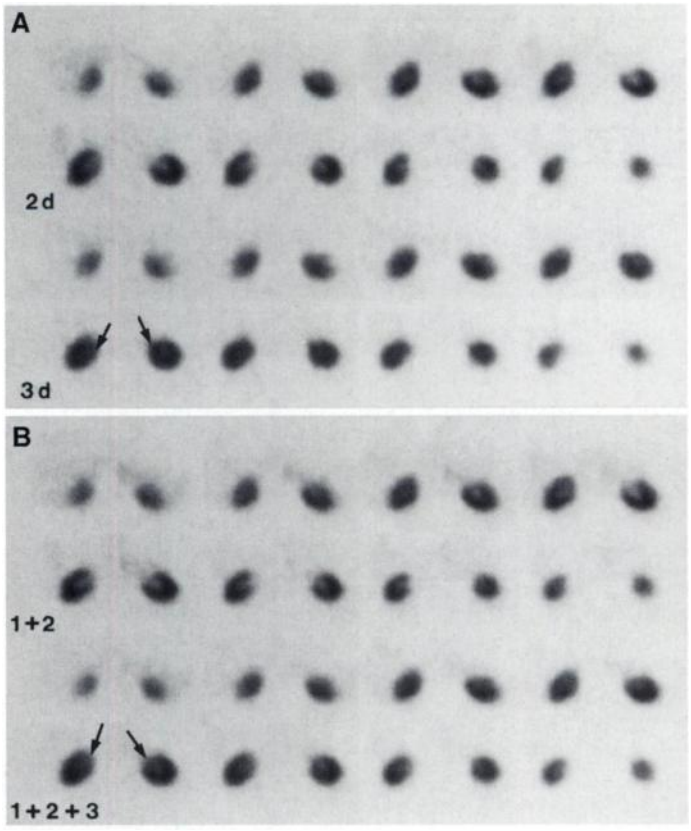

FIGURE 1. (A) Transaxial renal MAG3 SPECT images in a normal adult volunteer were reconstructed from the second (upper panel) and third minute (lower panel) of the acquisition sets. Slice thickness is 1 cm (3 pixels). Arrows indicate activity inside the drainage system. (B) Transaxial MAG3 SPECT images reconstructed from the initial 2-min (upper) and 3-min acquisition sets (lower).

Fast dynamic ECT acquisition was performed for 4 min at one revolution per minute (120° rotation for each one of the three detectors) in a continuous noncircular mode with 3° angular bins. Low-energy ultra-resolution collimators were used. The acquisition matrix was 128 × 64 (16 bits/pixel). Data for each minute were acquired and stored individually to obtain four 1-min datasets.

After the 4-min SPECT acquisition period, the current protocol of MAG3-SPECT provided three options: (a) when a patient was evaluated for renal parenchymal disorders exclusively (e.g., to rule out acute pyelonephritis), the study was concluded at 4 min; (b) when general information about kidney drainage was also needed,

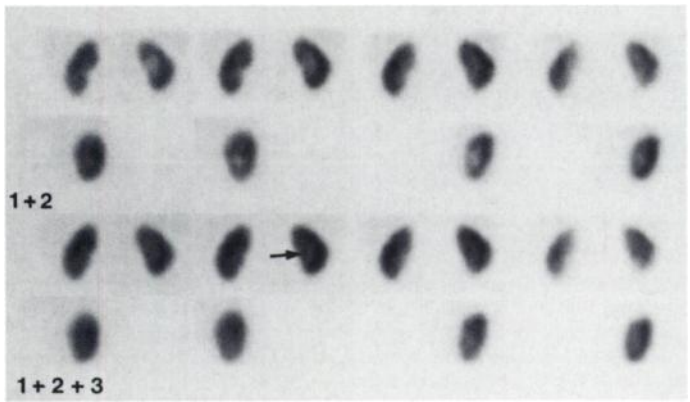

FIGURE 2. Coronal and sagittal MAG3 SPECT images reconstructed as in Figure 1B: upper panel, 1 + 2 min; lower panel, 1 + 2 + 3-min sets. Arrow indicates activity within the drainage system.

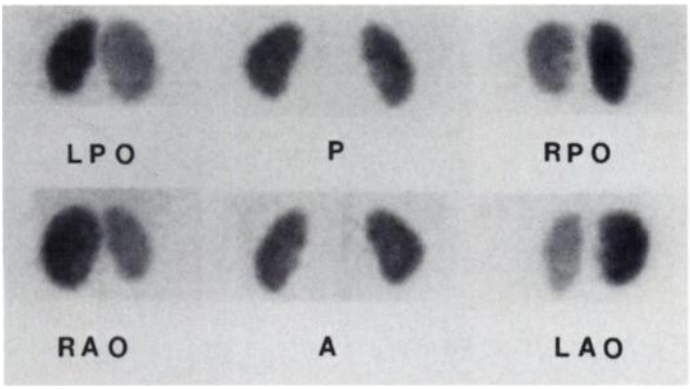

FIGURE 3. Selected views from the 36 reprojection (RPJ) images of the volume-rendered MAG3 SPECT/RPJ, which was reconstructed after grouping the initial 3-min acquisition datasets of the same study as shown in Figures 1 and 2.

the patient remained in the laboratory and a static image was obtained with a planar camera at 20 min postinjection; and (c) when diuretic renography was also indicated, the investigation continued for an additional 18 min in planar dynamic mode and posterior projection using one detector of the SPECT camera (*21*).

The above SPECT acquisition protocol provided four 1-min sets of raw data corresponding to the 4-min acquisition period. Reconstruction was performed for each one of the four 1-min raw data sets individually and for two grouped raw data sets obtained during: (a) the initial 2 min of the acquisition period (1 min + 2 min sets) and (b) the initial 3 min (1 min + 2 min + 3 min sets). Reconstruction of these grouped sets was performed after the corresponding projections from each revolution were added appropriately, two or three together, to form new ECT sets.

A three-point slice smoothing was applied with coefficients [1 3 1]. A Hamming filter with 1.20 cycles/cm high cutoff frequency (2.247 cycles/cm Nyquist) was used. Reconstructed slices were in a 128 × 128 (16 bits per pixel) mode. Attenuation correction was applied. Transaxial, coronal and sagittal slices were reconstructed in 1-cm thickness. The images were not reoriented because it was not needed for this study. Finally, volume-rendering, standard reprojection images (RPJ) were generated from the 3-min grouped SPECT data (*22*). Studies were reviewed on the computer display.

TABLE 1
Renal Parenchymal Counts and Kidney-to-Background Ratios

	Planar MAG3 (total kidney)*		SPECT-MAG3 (1-cm thick slice)†	
	Adult	Newborn	Adult	Newborn
1st min	110 (2.4)	23 (1.4)	100 (3.5)	8 (3)
2nd min	205 (3.4)	27 (2.3)	180 (12)	20 (4)
3rd min	240 (4.7)	28 (3)	230 (18)	25 (6)
4th min	260 (5.1)	21 (3)	Not useful	25 (7)
1 + 2 min	315 (3)	50 (2)	280 (9)	26 (3)
1 + 2 + 3 min	554 (4)	78 (2.5)	510 (15)‡	56 (4)

*Representative total kidney counts (in thousands) after administration of 10 mCi of MAG3 in one adult and 1 mCi in one newborn. Kidney-to-background (circumferential) ratios are in parentheses. Patients had normal renal function by creatinine levels and MAG3 scintigraphy. General-purpose collimators, Picker Dyna Camera (Cleveland, OH).

†The counts (in thousands) of a 1-cm thick SPECT slice (center of kidney) after injection of 20 mCi MAG3 in an adult and 2 mCi in a newborn. The kidney-to-background (circumferential) ratios are in parenthesis. Ultra-resolution collimators, Trionix (Twinsburg, OH).

‡When 6 mCi of DMSA was used in this adult patient for DMSA SPECT, corresponding values were 1,700 (46). Ultra-resolution collimators, Trionix.

RESULTS

SPECT images reconstructed from either the second- or third-minute raw data sets (Fig. 1A), and from grouped data of either the initial 2 or 3 min of acquisition (Fig. 1B and Fig. 2) visualized the renal parenchyma with acceptable clarity, contrast and detail. The distribution of the activity in the renal parenchyma (cortex and medulla) was uniform by visual evaluation. SPECT images reconstructed from the grouped data

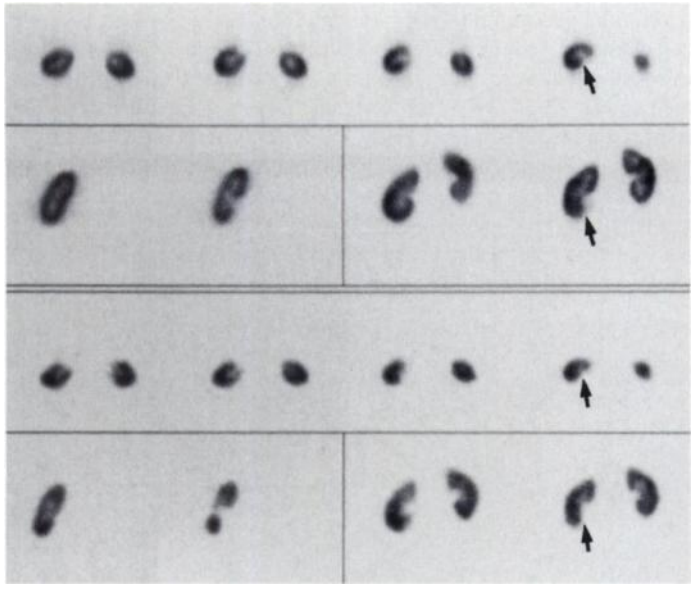

FIGURE 4. SPECT renal studies in an adult volunteer with a past history of pyelonephritis and a small defect in the lower pole of the right kidney postero-medially (arrows). Upper two rows: Transaxial, sagittal and coronal DMSA SPECT images reconstructed from 30-min acquisition data 4 hr after injection of 6 mCi DMSA (stop-and-shoot, 20 sec/view, 120° × 3 rotation, 5°/stop). Lower two rows: Corresponding MAG3 SPECT images reconstructed from the grouped initial 3 min of the acquisition datasets after injection of 20 mCi MAG3. Both studies were acquired and reconstructed with the same camera/collimator/computer system.

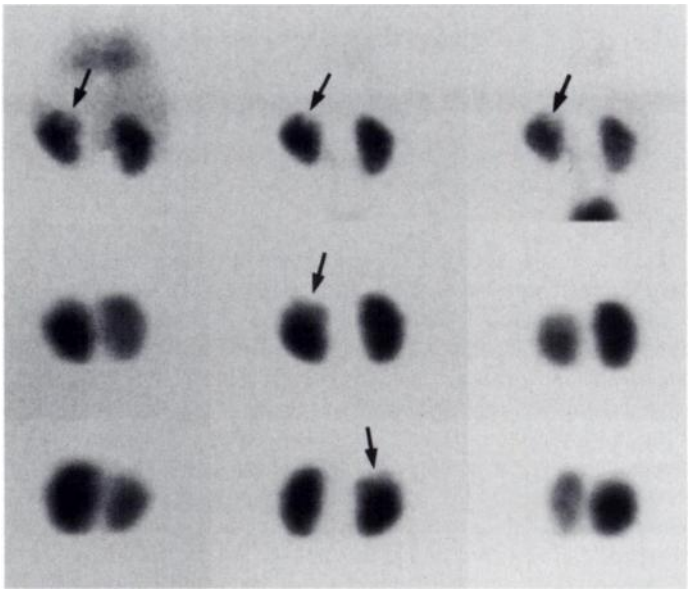

FIGURE 5. Renal MAG3 studies in a 6-mo-old infant with first UTI. Top: Routine planar posterior sequential 2-min images obtained with an all-purpose collimator. These are the first three postinjection images. Middle and bottom: SPECT/RPJ images (next day). Selected projections as in Figure 3. Both studies showed that the upper pole of the left kidney was not functioning (without volume loss), which is compatible with acute pyelonephritis (arrows).

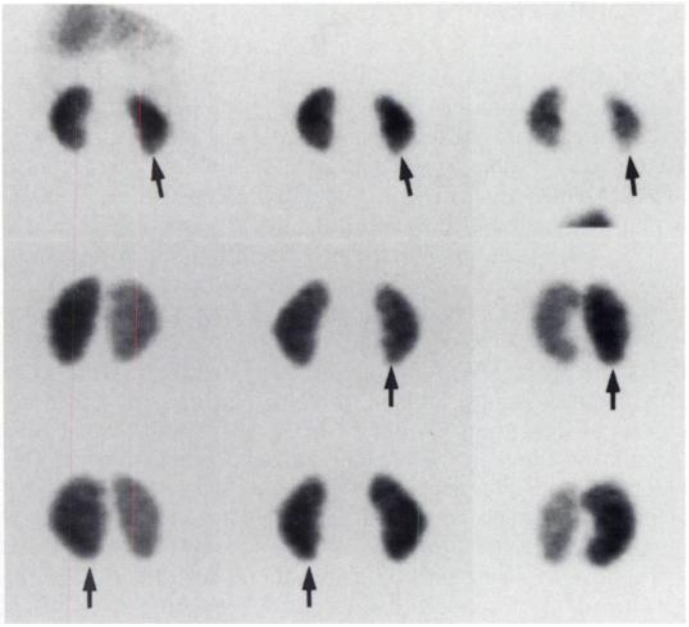

FIGURE 6. Renal MAG3 studies in an infant with UTI. Top: Planar images acquired as in Figure 5. A small area with decreased activity of questionable significance is visible in the right lower pole (arrow). Middle and bottom: SPECT/RPJ images (2 days later, selected projections as in Fig. 3) indicate no abnormality in the region, which appears slightly thinner than the contralateral lower pole.

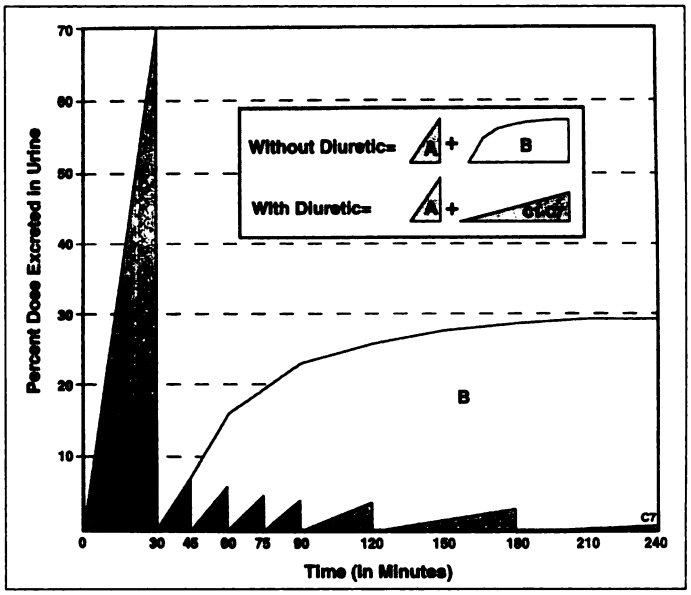

FIGURE 8. Diagram of the percent injected dose of MAG3 accumulated in the bladder compared with time of residence. Area A is the same without or with induced diuresis. The entire Area B applies to patients without diuretic. Furosemide, however, resulted in a much lower residence time, as indicated by the small spikes at the bottom (C_1-C_7). Bladder exposure, a factor of the area under the curve, is greater (× 3) without diuretic (A + B) than after furosemide (A + C_{1-7}).

were of better quality because of a higher count density. However, the third-minute data (either alone or grouped with the first and second minute), showed activity in the deeper layers of the parenchyma (medulla and peripheral portions of calices) and, occasionally, in the central collecting system including the pelvis (Figs. 1, 2). The renal parenchymal images were evaluated in transaxial (Fig. 1), coronal and sagittal projection (Fig. 2). In addition, volume-rendered RPJ images generated from the initial 3-min grouped SPECT data were useful in providing an easily comprehensible three-dimensional impression of the functioning renal parenchyma (Fig. 3).

MAG3 SPECT images reconstructed individually from the first or fourth sets of the 1-min sequential raw data could not be used because of low count density in the first set, and interference by the drainage system, which was prominent in the fourth set. In this group of patients with normal renal function, the fourth-minute data were not useful and were not used for parenchymal imaging. However, the first-minute data were useful when grouped with the second- and third-minute acquisition sets, as described above.

In comparison with DMSA SPECT in the adult volunteer who had been studied previously with the same camera, MAG3 SPECT images of the renal parenchyma were of somewhat inferior quality (because of lower contrast with the background and less sharp edge definition), but equally diagnostic (Fig. 4, Table 1).

In the children, MAG3 SPECT studies provided clinically useful information. These compared favorably with planar MAG3 and GH SPECT studies performed within 4 days. Specifically, in two infants, MAG3 SPECT confirmed the existence of focal parenchymal lesions compatible with acute pyelonephritis, as planar images indicated (Fig. 5) and, in another infant, MAG3 SPECT clarified that the kidney was normal even though the planar MAG3 study was suspicious (Fig. 6). In a toddler with a suboptimal GH SPECT study, MAG3 SPECT provided diagnostic images and accurate split

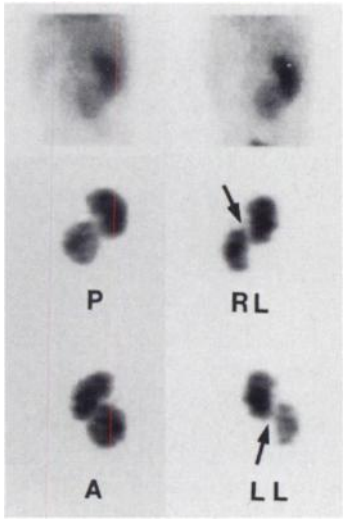

FIGURE 7. MAG3 studies in an asymptomatic newborn with a history of an ectopic kidney found on perinatal ultrasonography. Top: planar images obtained as in Figure 5. Middle and bottom: SPECT/RPJ selected images indicating the lack of fusion of the two kidneys (arrows). Split renal function by SPECT was calculated as 45% for the ectopic kidney in contrast to 30% by planar imaging. The greater attenuation (spine, more anterior position) of the ectopic kidney on the planar posterior image was the reason for the lower value.

TABLE 2
Radiation Dose Estimates for DMSA, GH and MAG3

Tissue	rem/6mCi DMSA	rem/20mCi GH	rem/10mCi MAG3 without diuretic	rem/20mCi MAG3 with IV diuretic
Bone marrow	0.13	0.13	0.018	0.036
Total body	0.09	0.20	0.024	0.048
Kidney	3.78	3.40	0.14	0.28
Bladder wall	0.42*	5.60/2.40†	1.7‡	1.13§
Testes	0.04*	0.26/0.16†	0.059‡	0.04§
Ovaries	0.08*	0.40/0.26†	0.086‡	0.06§

*Assumed bladder void at 4 hr (MIRD Pamphlet No. 1, 1968).
†Assumed bladder voids at 4 hr/or 2 hr (MIRD Pamphlet No. 11, 1975).
‡Assumed bladder voids at 30 min and 4 hr [Stabin et al. (25)].
§Furosemide-induced diuresis; bladder voids at 30 min and subsequently at frequent intervals (see Appendix).

renal function quantitation values for both the normal and the contralateral kidney with arrested growth, without interference from drainage system activity, which had complicated the GH study. Finally, in the newborn infant with an ectopic kidney, MAG3 SPECT identified the location of the kidneys and their split renal function more accurately than planar imaging (verified by phantom studies) and provided evidence that the kidneys were not fused (Fig. 7).

After hydration and under the effect of the diuretic, the five adult volunteers emptied their bladders at 30 min (or earlier) and at frequent intervals thereafter, which varied between 15 and 30 min for the first 2 hr and were no longer than 1 hr for the next 2 hr. Infants emptied their bladders between 10 to 15 min and again between 20 to 30 min postinjection and they followed a pattern similar to the adults thereafter. Based on our data of diuretic-induced frequent bladder voiding, a reduction in radiation dose estimates for the bladder wall and the gonads was calculated down to approximately 1/3 of the levels estimated from the same dose of MAG3 without a diuretic (Fig. 8, Table 2, Appendix).

DISCUSSION

DMSA is considered to be the best renal parenchymal imaging agent followed by GH. However, both require a waiting period of at least 3–4 hr after injection, an acquisition time of no less than 30 min and effective immobilization or sedation of the patient. Radiation exposure target organ for both radiopharmaceuticals is the kidney or the bladder wall for GH under certain voiding assumptions (Table 2).

Technetium-99m-MAG3 is a renal radiopharmaceutical with properties that make it suitable for dynamic studies. It appears, especially from data in the rat (*23*), that it is filtered only 2%–5% per pass because it is strongly protein bound. However, in both the rat (*23*) and the human (*24*), it is excreted actively by proximal tubular cells at a high rate of 55%–60% per pass. After an intravenous administration as a bolus, a large amount of injected MAG3 activity quickly accumulates and travels through the cortex into the medulla and the intrarenal drainage system and finally into the ureter. In the normal kidney, this is usually accomplished within the first 4 to 5 min after injection.

Due to the high extraction efficiency (60%) and the dramatic double exponential initial decline in plasma activity, a substantial contrast between the renal parenchyma and the background is generated during this early period (Table 1). During the first 4 min after injection, however, great variations in the renal parenchymal counts occur. These variations are expressed diagramatically by the renogram, which shows pronounced changes in the count rate during this period. Nevertheless, these 4 min are the most suitable for acquisition of SPECT data because the highest count rates and target-to-nontarget ratios occur during this time. To compensate for the lack of uniformity in parenchymal activity, a repeated rapid acquisition in 1-min sequential intervals for 4 min was used in this study. The kidneys were imaged repeatedly in 1-min intervals by a 360° acquisition mode (120°/detector) and, for each minute, a separate SPECT study was produced, resulting in uniform parenchymal activity by visual evaluation.

Finally, to acquire a sufficient number of counts and after careful evaluation of clinical data (Table 1), it became apparent that a minimum of 20 mCi MAG3 in the adult and a graduated dose of 2–20 mCi in the infant and child (0.3 mCi/kg, minimum 2 mCi) were needed for MAG3 SPECT. The recommended dose for MAG3, however, is 10 mCi and the radiation exposure target organ the urinary bladder (Table 2). One may observe, though, that for the total body, the bone marrow and the kidney, the exposure from 20 mCi MAG3 is less than from the recommended dose of DMSA or GH (Table 2). In addition, the administration of a diuretic-accelerated drainage system and bladder emptying, thus reducing radioisotope residence and radiation exposure of these organs to levels below those from 10 mCi dose (Table 2, Appendix).

For the model used in the Appendix, a constant monoexponential elimination of MAG3 in the urine was assumed that is an oversimplification. The frequent voiding after 30 min was observed in a small group of well-hydrated and appropriately instructed normal volunteers and may vary in the clinical environment. On the other hand, in infants the diuretic resulted in faster emptying of the bladder (usually at 10 min and also at 20–30 min postinjection). In addition, the diuretic effect increases bladder volume, dilutes MAG3, reduces the conversion electron radiation to the bladder wall and further reduces the radiation dose, in a manner not considered here. Therefore, the estimates are approximations and more precise modeling is required for accurate values.

The image quality and clinical usefulness of MAG3 SPECT, performed as described above, was acceptable in the five normal adults (Figs. 1–3). In the five children, it was superior to planar MAG3 (Figs. 5, 6) and to SPECT GH; SPECT MAG3 was somewhat inferior to DMSA SPECT (Fig. 4), because of the latter's higher count density and contrast with the background (Table 1), however, the clinical information was sufficient to make the diagnosis.

The advantages of three-dimensional imaging (MAG3 SPECT) in determining split renal function as compared to planar MAG3 were also evident in the neonate with the ectopic kidney (Fig. 7). DMSA SPECT split renal function quantitation has been reported (*26*) and results of phantom studies in our institution proved the accuracy of similar MAG3 SPECT quantitations.

The greatest advantage of MAG3 SPECT is the short duration of the test, which requires no waiting period after injection and is acquired within 4 min. Immobilization is easier for this short period of time and sedation is not needed.

While reconstruction time may be somewhat longer than the time required for DMSA SPECT, this is not a major concern with the availability of fast computers. Multidetector cameras are used in many hospitals for multipurpose applications (cardiac, bone, tumor, etc.).

In patients with a slight decrease in renal function, the fourth-minute acquisition data may also be used for parenchymal imaging because visualization of the drainage system would be delayed in such cases. In renal insufficiency, longer acquisition periods may be necessary in either multiple 1-min sets or in longer duration sets. Finally, the protocol provides for cases in which obstruction may be a concern; either a static image may be obtained at 20–25 min with a planar camera, or a diuretic renography may follow the MAG3 SPECT session to generate a comprehensive renal study (*21*). With increasing clinical experience and systematic use, adjustments of this technique may prove useful.

CONCLUSION

MAG3 SPECT of the renal parenchyma is feasible in children and adults with normal renal function and provides diagnostic information of focal disease and quantitative data for renal function. The higher than usual dosage of MAG3 required results in similar to a standard dose of DMSA or GH radiation exposure of the total body, bone marrow and kidneys. When combined with furosemide, exposure of the bladder wall, testes and ovaries does not exceed that of the standard dose. The

greatest advantage of this technique is that it allows the completion of the study of the renal parenchyma within only 4 min after injection. Further experience on sensitivity and specificity is required to establish and justify this procedure.

ACKNOWLEDGMENT

This work was presented in part at the annual meeting of the Southeastern Chapter of the Society of Nuclear Medicine, October 20–22, 1995 in Orlando, FL and at the 37th Annual Meeting of the Society of Nuclear Medicine, June 3–7, 1996 in Denver, CO.

APPENDIX

Estimation of Bladder Exposure When MAG3 Is Injected with Furosemide

It is known that 70% of the injected dose of MAG3 is found in urine 30 min after the injection (*15*). Assuming exponential rate of elimination of MAG3 in the urine, 70% of the 30% (21% of the original dose) will also be in the urine by the next 30 min and this will continue until all the radioactivity is excreted.

When the patients empty their bladders at 30 min per protocol (irrespective of the use of furosemide), bladder exposure during this period is a function of the area underneath the 30-min curve (Fig. 8, Area A).

Data without administration of a diuretic were compiled and published assuming voiding at 30 min and then at 4 hr (*25*). Such calculations provided estimates of bladder exposure that were based on the exposure times indicated in Figure 8 as the area under A plus the area under the continuous curve, B.

When 40 mg of furosemide was administered after hydration, adults emptied their bladders at 30 min by protocol and the Area A still applied. Under the effect of diuresis, however, bladder voiding occurred not only at 30 min but also at 45, 60, 75, 90, 120, 180 and 240 min, based on our data. This resulted in avoiding the exposure that is a factor of Area B and sustaining only the limited exposure that is a factor of the small shaded regions C_{1-7} (Fig. 8).

On the basis of this model we find (approximately):

(Area with diuretic)/(Area without diuretic) = 1/3

REFERENCES

1. Handmaker H, Young B, Lowenstein J. Clinical experience with Tc-99m-DMSA (dimercaptosuccinic acid): a new renal imaging agent. *J Nucl Med* 1975;16:28–32.
2. Leonard JC, Wenzi MDE, Allen W, et al. Gluceptate renal imaging: experience in a pediatric population. *Clin Pediatr* 1980;19:615–619.
3. Handmaker H. Nuclear renal imaging in acute pyelonephritis. *Semin Nucl Med* 1982;12:246–253.
4. Traisman FS, Conway JJ, Traisman HS, et al. The localization of urinary tract infeciton with Tc-99m-glucoheptonate scintigraphy. *Pediatr Radiology* 1986;16:403–406.
5. Sty JR, Wells RG, Schroeder BA, Starshak RJ. Diagnostic imaging in pediatric renal inflammatory disease. *JAMA* 1986;256:895–899.
6. Rushton HG, Majd M, Chandra R, Yim D. Evaluation of ^{99m}Tc-dimercaptosuccinic acid renal scan in experimental acute pyelonephritis in piglets. *J Urol* 1988;140:1169–1174.
7. Bjorgvinsson E, Majd M, Eggli KD. Diagnosis of acute pyelonephritis in children: comparison of sonography and ^{99m}Tc-DMSA scintigraphy. *Am J Roentgenol* 1991; 157:539–543.
8. Majd M, Rushton HG. Renal cortical scintigraphy in the diagnosis of acute pyelonephritis. *Semin Nucl Med* 1992;22:98–111.
9. Williams DE. Renal single-photon emission computed tomography: should we do it? *Semin Nucl Med 1992;*22:112–121.
10. Ziessman HA, Balseiro J, Fahey FH, et al. Technetium-99m-glucoheptonate for quantitation of differential renal function. *Am J Roentgenol* 1987;148:889–893.
11. Kawamura J, Hosokawa S, Yoshida O. Renal function studies using ^{99m}Tc-dimercaptosuccinic acid. *Clin Nucl Med* 1979;4:39–46.
12. Jacobson AF, Matsuoka DT, Ferency GF, et al. Comparison of scintigraphic renal differentials using radiolabeled orthoiodohippurate and glucoheptonate. *Clin Nucl Med* 1991;16:389–393.
13. O'Reilly PH, Pollard AJ. Nephroptosis: a cause of renal pain and a potential cause of inaccurate split renal function determination. *Br J Urol* 1988;61:284–288.
14. Groshar D, Frankel A, Iosilvesky G, et al. Quantitation of renal uptake of technetium-99m-DMSA using SPECT. *J Nucl Med* 1989;30:246–250.
15. Taylor A, Eshima D, Frizberg AR, et al. Comparison of I-131-OIH and Tc-99m-MAG3 renal imaging in volunteers. *J Nucl Med* 1986;27:795–803.
16. Eshima D, Taylor A Jr. Technetium-99m mercaptoacetyl-triglycine: update on the new ^{99m}Tc renal tubular function agent. *Semin Nucl Med* 1992;22:61–73.
17. Gordon I, Anderson PI, Lythgoe MF, Orton M. Can Technetium-99m-mercaptoacetyli-triglycine replace technetium-99m-dimercaptosuccinic acid in the exclusion of a focal renal defect? *J Nucl Med 1992;*33:2090–2093.
18. Piepsz A, Pintelon H, Verboven M, et al. Replacing ^{99m}Tc-DMSA for renal imaging [Abstract]? *Nucl Med Commun* 1992;13:494–496.
19. Sfakianakis GN, Aboud A, Cavagnaro F, et al. The role of dynamic MAG3 scintigraphy in the diagnosis of acute pyelonephritis, a comparison with DMSA [Abstract]. *J Nucl Med* 1993;34:117P.
20. Sfakianakis GN, Zilleruelo G, Cavagnaro F, et al. A prospective comparative DMSA and MAG3 study in acute pyelonephritis. In: Taylor A, Nally JV, Thompson H, eds. *Radionuclides in nephrourology.* Reston, VA: Society of Nuclear Medicine: 1997: in press.
21. Sfakianakis GN, Georgiou M, Cavagnaro F, et al. Fast protocols for obstruction (diuretic renography) and for renovascular hypertension (ACE Inhibition). *J Nucl Med Technol* 1992;20:193–206.
22. Talton DA, Goldwasser SM, Reynolds RA, et al. Volume rendering algorithms for the presentation of 3D medical data. *Proc Vol. III: NCGA Computer Graphics 8th Annual Conference.* Fairfax, VA: National Computer Graphics Association; 1987;119–124.
23. Mullez-Suur R, Mullez-Suur C. Glomerular filtration and tubular secretion of MAG3 in the rat kidney. *J Nucl Med* 1989;30:1986–1991.
24. Bubeck B, Brandau W, Weber E, Kalbe T, Parekh N, Georgi P. Pharmacokinetics of technetium-99m-MAG3 in humans. *J Nucl Med* 1990;31:1285–1293.
25. Stabin M, Taylor A Jr, Eshima D, et al. Radiation dosimetry for technetium-99m-MAG3, technetium-99m-DTPA and iodine-131-OIH based on human biodistribution studies. *J Nucl Med* 1992;33:33–40.
26. Groshar D, Issaq E, Nativ O, Livne P. Increased renal function in kidneys with ureteropelvic junction obstruction: fact or artifact? Assessment by quantitative single-photon emission computerized tomography by dimercapto-succinic acid uptake by the kidneys. *J Urol* 1996;155:844–846.